Surfatron Acceleration of Ions by Fast Magnetosonic Shocks generated during Two Current Loops Coalescence

Laboratory for Plasma Astrophysics, Faculty of Engineering
Shinji Saito and Jun-ichi Sakai
d023008@ems.toyama-u.ac.jp

We investigate the coalescence process of two parallel current loops with co-helicity by using two dimensional, electromagnetic, relativistic Particle-In-Cell (PIC) code. We found that in a later stage of the two current loops coalescence, fast magnetosonic waves are generated as a result of rebound of the coalescence and they develop to shock waves propagating away from the coalesced loops. We also found that near the fast magnetosonic shock front the ions can be promptly accelerated by the surfatron acceleration mechanism. We apply the obtained simulation results to the proton acceleration during solar flares.
Keywords : acceleration of particles, shock waves, Sun-flares, Sun-magnetic field

1 Introduction

In most strong flare events the time profile of the prompt gamma-ray line emission caused from energetic protons is observed to be very similar to that of the bremsstrahlung hard X-rays emitted by energetic electrons (Aschwanden 2002). This suggests that the acceleration and propagation of the flare-accelerated protons and electrons are closely related. The most typical event among them is the 1980 June 7 flare observed by the SMM (Forrest and Chupp 1983), which flare was explained by the current loop coalescence model (Tajima et al. 1982; Sakai & Ohsawa 1987; Sakai & De Jager 1996). Sakai & de Jager (1996) gave a review of the high-resolution observations of solar plasma loops with simulations of current-carrying loops and tried to arrive at the understanding of solar flare phenomena.

However, the location, size and geometry of the accelerated proton collision region remains unknown until now. Recent paper by Hurford et al. (2003) presents the first gamma-ray images of a solar flare taken from the Reuven Ramaty High Energy Solar Spectroscopic Imager (RHESSI) for the X4.8 flare of 2002 July 23. The result shows that the centroid of the 2.223 MeV image was found to be displaced by 20 ± 6 arcsec from that of the 0.3-0.5 MeV, implying a difference in acceleration and /or propagation between the accelerated electron and proton populations near the Sun. The fact that proton-associated gamma-ray source does not coincide with the electron-bremsstrahlung sources suggests that the protons would be accelerated in one direction by the DC electric field and could subsequently interact in spatially separated sources. Therefore it is now important to investigate in details the proton acceleration processes for different types of flares.

In this paper we investigate the coalescence process of two parallel current loops with co-helicity by using two dimensional, electromagnetic, relativistic Particle-In-Cell (PIC) code. We found that in a later stage of the two current loops coalescence, fast magnetosonic waves are generated as a result of rebound of the coalescence and they develop to shock waves. We also found that near the fast magnetosonic shock front the ions can be promptly accelerated by the surfatron acceleration mechanism (Sagdeev & Shapiro 1973; Katsouleas & Dawson 1983; Ohsawa 1985; Ohsawa & Sakai 1987). We apply the obtained simulation results to the proton acceleration during solar flares.

In §2 we present our simulation model. In §3 we present our simulation results and in §4 we summarize our results and discuss applications to solar flares.

2 Simulation Model

We used 2D3V, fully relativistic electromagnetic particle-in-cell (PIC) code, modified from 3D3V TRISTAN code (Buneman 1993). The system size is $L_x = L_y = 900\Delta$, where $\Delta(= 1)$ is grid size. The free boundary conditions for both x and y directions are imposed on particles and fields. We considered that a single steady-state current loop satisfies the equilibrium condition in the form:

$$B_\theta = \frac{B_0 r/a}{1 + (r/a)^2} \tag{1}$$

$$B_z = \frac{B_0}{1 + (r/a)^2} \tag{2}$$

The two current loops are assumed to be in force-free state, respectively. The z component is perpendicular to the two dimensional plane. The center of two current loops is located at $(x_1, y_1) = (300\Delta, 300\Delta)$ for the first loop and at $(x_2, y_2) = (600\Delta, 600\Delta)$ for the second loop. The radius, a of both loops is 100Δ. There are about 80 million uniformly distributed electron-ion pairs in the system, which are keeping the charge neutrality. The average numbers of electron-ion pairs in a cell is about 100 particles. Ion temperature is equal to the electron temperature. Only electrons are drifted as electric current of the loops. Other parameters are as follows : the time step $\omega_{pe}\Delta t = 0.05$, mass ratio $m_i/m_e = 16.0$, Debye length $v_{th,e}/\omega_{pe} = 1.0\Delta$, the collisionless skin depth $c/\omega_{pe} = 10\Delta$. The physical quantities associated with the magnetic field B_0, like the ratio of ω_{ce} to ω_{pe}, plasma beta, electron Larmor radius, and ion Larmor radius are 0.8, 0.015, 1.25Δ, and 5Δ, respectively.

3 Simulation Results

First of all we show how the magnetosonic waves are generated during two current loops coalescence in Figure 1. Figure 1(a.1-4) and (b.1-4) show the time development of the magnetic field B_z with the grayscales and averaged ion velocity $v_{xy,i}$ with the vector plots, respectively, at $\omega_{pe}t$ =0, 200, 250, and 300. The horizontal and the vertical axis show the x and y direction, respectively. In the initial state (Fig.2 (a.1) and (b.1)), the center of the magnetic field B_z is located at $(300\Delta, 300\Delta)$ for first loop and at $(600\Delta, 600\Delta)$ for second loop, and there are no plasma flows in the system. After time goes on, two current loops approach each other due to the attractive force caused by their electric currents. At $\omega_{pe}t = 200$, the magnetic fields are compressed due to the plasma flows behind the current loops, as seen in Fig.1(b.2). Therefore, the magnetic field energy in the compressed region may overcome the local kinetic energy, resulting in the energy conversion from the magnetic field energy to the kinetic energy of streaming plasma behind the loops. At $\omega_{pe}t = 250$, the pulse-like magnetosonic waves are generated behind the loops, which are shown by dashed circles in Fig.1(a.3). As seen in Fig.1(a.4), the waves propagate outwards in the direction anti-parallel to the plasma flows. The generated fast magnetosonic waves eventually develop to shock waves that play an important role for accelerating ions by the surfatron acceleration mechanism (Ohsawa & Sakai 1987). Next, we pay attention to the structure of the generated nonlinear magnetosonic wave. Figure 2 shows the vector plots

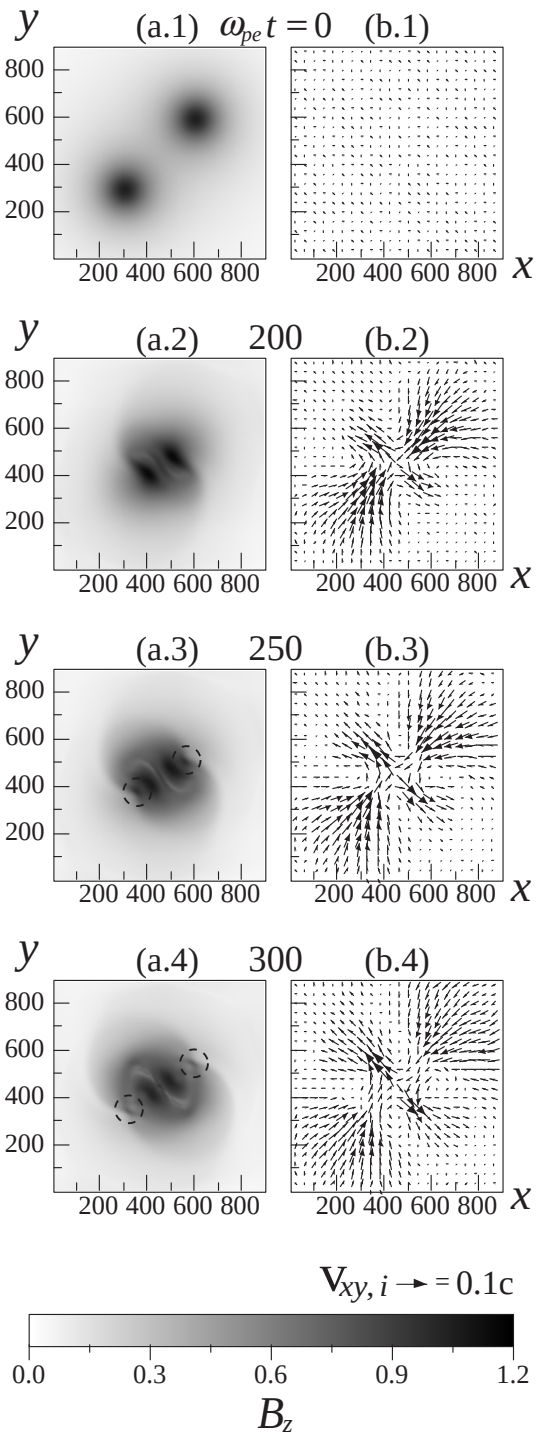

Figure 1: (a.1-4) and (b.1-4) show the time development of magnetic field B_z and averaged ion velocity, respectively, at $\omega_{pe}t$ =0, 200, 250, and 300. The dashed circles indicate the magnetosonic waves propagating to outer region.

and the intensity (grayscale) of the magnetic field B_{xy} (a.1-2) and the electric field E_{xy} (b.1-2), respectively, at $\omega_{pe}t$ =350 and 500. The plotted region is a part of the system; from 100Δ to 400Δ in the x-direction, and from 100Δ to 400Δ in the y-direction. In Fig. 2 (a.1-2), we can see that the compressed wave region propagates normal to the local magnetic field, as characterized by the nonlinear magnetosonic wave. As seen in Fig. 2 (b.1-2), the electric fields associated with the magnetosonic wave are generated normal to the wave front with the scale of the electron skin depth. The electric field strength

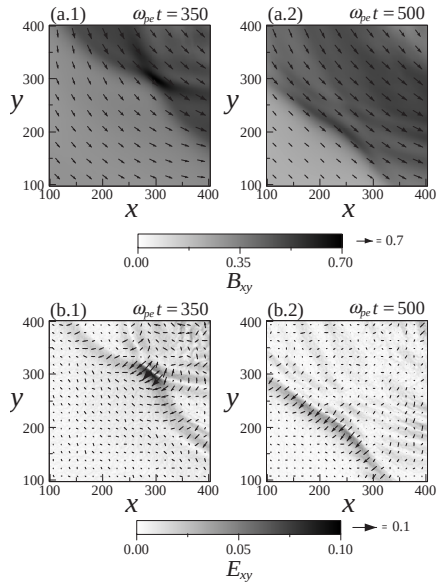

Figure 2: (a.1-2) and (b.1-2) show the vector plots overlapped with the intensity of magnetic field $B_{xy} = \sqrt{B_x^2 + B_y^2}$ and electric field $E_{xy} = \sqrt{E_x^2 + E_y^2}$, respectively, at $\omega_{pe}t$ =350 and 500. The plotted region is a part of the system; (100Δ − 400Δ) in the x-direction and (100Δ − 400Δ) in the y-direction.

normalized by magnetic field is calculated as

$$\frac{E}{B} \approx r_{L,i} \left(\frac{c}{\omega_{pe}} \right)^{-1} \frac{v_A^2}{c v_{th,i}} (M_A - 1)^{\frac{3}{2}} \qquad (3)$$

from the nonlinear theory of magnetosonic waves. Here, $r_{L,i}$, v_A, c, and M_A are the ion Larmor radius, Alfvén velocity, light velocity, and Alfvén Mach number, respectively. The Alfvén Mach number is calculated from the continuity equation as

$$M_A = \frac{v_{0,i} + v_{1,i}}{v_A} = \frac{n_{1,i}}{n_{0,i}} \left(1 - \frac{v_{0,i}}{v_A} \right) + \frac{v_{0,i}}{v_A}. \qquad (4)$$

Here, $v_{0,i}$, $n_{0,i}$, $v_{1,i}$, and $n_{1,i}$ are the ion bulk velocity, ion bulk density, the perturbations of ion velocity, and density, respectively. We assume that the phase velocity ω/k is equal to v_A. We can obtain $M_A = 1.75$ from above equation with averaged physical quantities between $\omega_{pe}t = 350$ and $\omega_{pe}t = 500$ around the wave front. By using this result, we estimate the intensity of electric field normal to the wave front, whose value agrees well with the simulation result. The generated electric field by the nonlinear effect of magnetosonic wave, normal to the wave front is important for the acceleration of ions, because the basic concept of the surfatron acceleration is $\mathbf{E} \times \mathbf{B}$ drift. Figure 3 shows the time development of ions in phase space at $\omega_{pe}t$ = (a) 200, (b) 350, and (c) 500, respectively. The horizontal and the vertical axis show the x-axis between 100Δ and 400Δ, and the ion velocity normalized by light velocity, respectively. At $\omega_{pe}t$ =200, there are no accelerated ions in the plotted region, while at $\omega_{pe}t$ =350 and 500 some ions are accelerated to the z-direction near the narrow region corresponding to the position of the magnetosonic shock front as shown in Fig.3. At $\omega_{pe}t$ =500, more ions are accelerated up to +0.2c. In the ion accelerated region, the electrons are not accelerated because the surfatron mechanism accelerates only ions for the condition as $\omega_{pe} > \omega_{ce}$ which condition is satisfied in the outer region away from the center of current coalescence region. Therefore the only trapped ions by the magnetosonic wave can be accelerated up to

$$\frac{v}{v_A} \approx \left(\frac{m_i}{m_e} \right)^{1/2} (M_A - 1)^{3/2}. \qquad (5)$$

by the surfatron acceleration mechanism. By using the mass ratio, m_i / m_e =16, and Mach number =1.75, we find that v/v_A becomes about 2.6. In the acceleration region, Alfvén velocity is about 0.08c. Therefore, the theoretical value of accelerated velocity in the region is 0.2c, which is a good agreement with the simulation result as seen in Fig. 3(c). Furthermore, as seen in Fig. 3, the time period for the acceleration is less than $\omega_{pe}\Delta T = 300$ which is correspond to $\omega_{ci}\Delta T = 6.0$, where ω_{ci} is determined by the intensity of magnetic field in the accelerated region. The theoretical value for the acceleration period is presented by the equation,

$$\omega_{ci} t \approx M_A^{-1} \frac{\omega_{pi}}{\omega_{ci}}. \qquad (6)$$

By using $M_A = 1.75$, and $\omega_{pi}/\omega_{ci} = 12.5$, we obtain that the time period for acceleration is $\omega_{ci}t \approx 7.1$, which shows also good agreement with our simulation result. The results obtained from our simulation indicate clearly that the ion acceleration near the shock front is caused by the surfatron mechanism. Some ions trapped by the electric fields associated with the magnetosonic shock wave can be accelerated to the direction perpendicular both to the local

magnetic field and to the propagation direction of the shock for the condition as $\omega_{pe} > \omega_{ce}$.

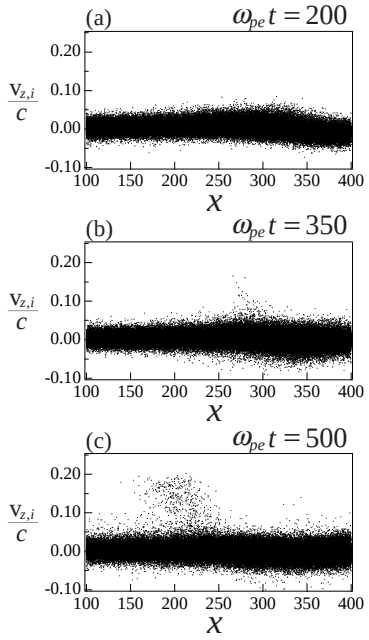

Figure 3: (a)-(c) show the time development of ions in phase space at $\omega_{pe}t$ =200, 350, and 500, respectively. Horizontal and vertical axis show the x-axis between 100Δ and 400Δ and ion velocity normalized by light velocity, respectively.

4 Summary

We investigated two current loops interaction with force-free magnetic field configuration, by using 2D3V, fully relativistic electromagnetic particle-in-cell code. We found that in a later stage of the two current loops coalescence, fast magnetosonic waves are generated as a result of rebound of the coalescence and they develop to shock waves propagating away from the coalesced loops. We also found that near the fast magnetosonic shock front the ions can be promptly accelerated by the surfatron acceleration mechanism. Some ions are accelerated by the surfatron mechanism for the condition of $\omega_{pe} > \omega_{ce}$ (Ohsawa & Sakai 1987), up to $v/v_A \approx (m_i/m_e)^{1/2} (M_A - 1)^{3/2}$. The simulation results for ion acceleration showed a good agreement with the theoretical results for the surfatron acceleration. The recent observation by the RHESSI satellite (Hurford *et al.* 2003) implied a difference in acceleration and/or propagation between the accelerated electron and ion populations near the Sun. We apply the surfatron mechanism to one of the proton acceleration mechanism in solar flares caused by current loops coalescence. Due to the above surfatron mechanism, the only protons are accelerated to one direction (in the present simulation, to the +z direction) in the region with the condition $\omega_{pe} > \omega_{ce}$, away from the current loops coalescence region. If we take the plasma parameters of the solar corona as $v_A \sim 10^8 cm/s$ and $m_i/m_e \sim 1836$, the accelerated proton velocity by the surfatron mechanism with the Alfén Mach=1.7 which is obtained from the simulation is $v_{acc,i} \sim 2.5 \times 10^9 cm/s$, which corresponds to the kinetic energy $1/2 m_i v_i^2 \sim 3.5$ MeV. This energy is enough to provide the observed accelerated proton energy.

Acknowledgment

We would like to thank Prof. Y. Ohsawa for useful discussions on the surfatron acceleration. S. Saito is supported by research fellowship of the Japan Society for the Promotion of Science (JSPS) for young scientists, as JSPS Research Fellow.

References

[1] Aschwanden, M.J. 2002, Space Sci. Rev. 101, Nos. 1-2, 1

[2] Buneman, O. 1958, Phys. Rev. Lett., 1, 8

[3] Buneman, O. 1993, in Computer Space Plasma Physics, Simulation Techniques and Software, edited by H. Matsumoto & Y. Omura, Terra Scientific, Tokyo, p.67

[4] Forrest, D.J. & Chupp, E. L. 1983, Nature 305, 291

[5] Hurford, G.J., Schwartz, R.A., Krucker, S., Lin. R.P., Smith, D.M., & Vilmer, N. 2003, ApJ, 595, L77

[6] Katsouleas, T. & Dawson, J. M. 1983, Phys. Rev. Lett. 51, 392

[7] Ohsawa, Y. 1985, Phys. Fluids, 28, 2130

[8] Ohsawa, Y. & Sakai, J. I. 1987, ApJ. 313, 440

[9] Sagdeev, R. Z. & Shapiro, V. D. 1973, JETP Letters, 17, 279

[10] Sakai, J.I. and de Jager, C. 1996, Space Sci. Rev., 77, 1

[11] Sakai, J.I. & Ohsawa, Y. 1987, Space Sci. Rev. 46, 113

[12] Tajima, T., Brunel, F. & Sakai, J.I. 1982, ApJ, 245, L45